Process Biochemistry 147 (2024) 31–38

Contents lists available at ScienceDirect

Process Biochemistry

journal homepage: www.elsevier.com/locate/procbio

Biosynthesis and in vivo wound healing abilities of *Dactyloctenium aegyptium*-mediated silver nanoparticles used as hydrogel dressing

Maryam Zain [a], Sana Nayab [a], Zermina Rashid [b,d,*], Ambreen Aleem [c], Hina Raza [c], Mohamed Deifallah Yousif [d,**]

[a] Department of Biochemistry and Biotechnology, The Women University Multan, Multan, Pakistan
[b] Department of Pharmacy, The Women University Multan, Multan, Pakistan
[c] Faculty of Pharmacy, Bahauddin Zakariya University, Multan, Pakistan
[d] UCL School of Pharmacy, University College London, London, UK

ARTICLE INFO

Keywords:
Green synthesis - *Dactyloctenium aegyptium* - silver nanoparticles - antibacterial activity - hydrogel dressing - wound healing

ABSTRACT

Wounds offer a medium for the growth of pathogens and their entry into the body, which necessitates effective wound healing treatments. Herein, we report the green synthesis of silver nanoparticles (AgNPs) using *Dactyloctenium aegyptium* extract as a capping and reducing agent for wound healing applications. The synthesized nanoparticles were characterized by UV-Vis, FT-IR, SEM, XRD, and in vitro antibacterial activity. Nanoparticles were then incorporated into PVA, Na-alginate, and gelatin-based hydrogel dressings to investigate their in vivo wound healing capability in rats. The color change of the reaction mixture and the surface plasmon resonance (400 nm) confirmed the formation of AgNPs. FT-IR analysis revealed the involvement of plant extract phytochemicals in the capping and stabilization of nanoparticles. The nanoparticles were crystalline in nature, with an average crystallite size of 28.03 nm and exhibited antibacterial activity against *S. aureus*, *P. aeruginosa*, *K. pneumoniae* and *E. coli* (ZOI 19 ± 0.0, 9 ± 0.0, 13 ± 0.0, and 13 ± 0.0 mm respectively). Furthermore, silver nanoparticle-loaded hydrogels showed accelerated wound healing in rats compared to untreated rats and rats treated with a commercial product. Thus, the developed hydrogel dressing has the potential for clinical application in wound healing and infection treatment.

1. Introduction

Wounds are tissue injuries caused by physical or thermal damage and are subjected to bacterial infections that can hinder the healing process [1]. The wound healing process involves the restoration of devitalized cellular structures and tissue layers, thus requiring a suitable platform for wound management, with the primary objectives of rapid wound closure and minimum scar formation [2]. Among the different commercially available wound care products, hydrogels and hydrocolloid-based wound dressings have been primarily formulated for the management of moist wounds. These formulations allow the exchange of gases, provide a barrier to microbial penetration, and remove excess exudate [3]. For accelerated wound healing, an ideal wound dressing should have the ability to maintain a constant temperature, favor the healing process, possess antimicrobial activity, and protect new cells [4].

Nanotechnology has fueled tremendous progress in material science, allowing for the creation of novel products by manipulating matter at the nanoscale level. Metallic nanoparticles (1–100 nm) have unique properties, and their effectiveness in fighting infectious diseases is an exciting field of research with extensive applications [5]. Furthermore, metallic nanoparticles have been reported to possess antioxidant, anticancer, antidiabetic, pollutant chelation, photocatalytic, and glucose-sensing activities [6-9]. Among metallic nanoparticles, silver nanoparticles (AgNPs) are widely used in medicine, pharmaceuticals, and agriculture. The physical and chemical processes used for AgNP synthesis are complex and expensive, involving harmful solvents that leave behind toxic residues and by-products that have adverse effects on the ecosystem [10]. Conversely, Phyto-nanotechnology (the biosynthesis of metallic nanoparticles using plant extracts) offers a simple, less time-consuming, eco-friendly, cost-effective, and easily scalable alternative route for their synthesis [11,12].

* Corresponding author at: Department of Pharmacy, The Women University Multan, Multan, Pakistan.
** Corresponding author.
E-mail addresses: zermina.6371@wum.edu.pk (Z. Rashid), mohamed.yousif@ucl.ac.uk (M.D. Yousif).

https://doi.org/10.1016/j.procbio.2024.08.011
Received 31 December 2023; Received in revised form 11 August 2024; Accepted 12 August 2024
Available online 13 August 2024

Plant extracts are rich in bioactive compounds that are easily extracted by water and can act as reducing and capping agents in the biosynthesis of nanoparticles [13]. When they are used, their intrinsic characteristics and bioactivity are transformed into prepared nanoparticles. AgNPs have been synthesized using plant extracts and reported for their innate properties of antibacterial, anti-inflammation, antioxidation, and anticancer activities, as well as wound healing abilities [14,15]. *Dactyloctenium aegyptium* (*D. aegyptium*), commonly known as Durban crowfoot grass, belongs to the Poaceae family and has folkloric repute as an astringent and anthelmintic, and is used against many diseases such as smallpox, cough, gastric ulcers, urinary lithiasis, and wounds [16]. *D. aegyptium* is rich in carbohydrates, amino acids, proteins, alkaloids, terpenoids, flavonoids, tannins, phenols, steroids, and fixed oils [17]; therefore, it can be explored as a mediator for the green synthesis of AgNPs.

AgNPs can be incorporated into hydrogel dressings to facilitate faster wound healing [18]. Polymers such as polyvinyl alcohol (PVA), sodium alginate, and gelatin are suitable materials for the formulation of hydrogel dressings owing to their biocompatibility and nontoxicity. PVA is a synthetic polymer with excellent gel-forming capability and has been extensively used as a platform for wound dressing formulations [19–21]. However, PVA alone causes poor swelling and poor mechanical properties in wound dressings. Sodium alginate is a natural polymer composed of 1,4-linked D-mannuronic acid and L-guluronic acid residues that exhibit gelation attributes [22], which allows its wide application in tissue engineering and wound dressing. Gelatin is a protein that possesses relevant features of plasticity, adhesiveness, and suitability as a platform for tissue growth [23]. To the best of our knowledge, PVA, Na alginate, and gelatin have not been combined to form a hydrogel dressing for wound healing.

Herein, we describe the preparation of AgNPs using *D. aegyptium* aqueous extract. *D. aegyptium*-mediated silver nanoparticles (AgNPs-DA) were characterized using UV-Vis spectroscopy, FTIR, XRD, and SEM. As wounds could be a medium for bacterial growth and entry portal to the body, the in vitro antibacterial activity of the particles against *S. aureus*, *E. coli*, *K. pneumoniae*, and *P. aeruginosa* was also investigated. Furthermore, the optimized particles were incorporated into pH-responsive hydrogel dressings made from PVA, gelatin, and sodium alginate to evaluate the potential wound healing abilities of the nanoparticles.

2. Materials and methods

2.1. Materials

Silver nitrate ($AgNO_3$) was purchased from Carlo Erba Reagent (Germany). The Dactyloctenium *aegyptium* plant was freshly collected from the botanical garden of the Women's University of Multan, Multan, Pakistan. Polyvinyl alcohol (PVA; M. wt. 72,000), sodium alginate, and gelatin were purchased from Merck Pvt., Ltd. (Pakistan). All chemicals and reagents used were of analytical grade.

2.2. Plant collection and extract preparation

The freshly collected *Dactyloctenium aegyptium* plant (whole plant) was first washed with tap water three times, then with distilled water, air-dried under shade in the laboratory, and delicately ground. Plant powder (15 g) was boiled in 100 ml of deionized water for 15 min at 80 °C, filtered, and the filtrate was kept in a refrigerator at 4 °C until further use.

2.3. Silver nitrate precursor preparation

Silver nitrate was used as the precursor for the biosynthesis of silver nanoparticles (AgNPs) from the *D. aegyptium* aqueous extract. Silver nitrate solutions with different molarities (2.5 mM to 15 mM) were prepared by dissolving $AgNO_3$ powder in distilled water and stored at 4 °C for further use.

2.4. Synthesis of silver nanoparticles

Ten different batches of nanoparticles were prepared (S1 to S10) using the green synthesis method [24]. For the preparation of batches S1–S5, 50 ml of silver nitrate solution (10 mM) was added dropwise to varying concentrations of plant extract (Table 2). For the preparation of batches S6 to S10, 50 ml of silver nitrate solution of varying moralities (Table 2) was added dropwise to the 5 % plant extract. The reaction mixtures were heated (45 °C) with constant stirring for 45 min, the pH was maintained at 9. After 45 min of stirring, the colour of the reaction mixture changed from yellow to brown, indicating the successful synthesis of AgNPs-DA. The resultant suspension was centrifuged for 20 min at 7000 rpm, the supernatant was discarded, and the pellets were resuspended in distilled water and centrifuged again. The last procedure was repeated thrice to remove any contaminants. The resulting pellets were air-dried and stored in airtight containers for further investigation.

2.5. Characterization of AgNPs-DA

2.5.1. UV- visible spectrophotometer analysis

UV–visible spectroscopy is a useful technique for assessing the attributes of metallic NPs in colloidal dispersions. UV-Vis spectra of the formed AgNPs were recorded over a continuous wavelength region from 200 to 700 nm using a UV–visible spectrophotometer (PerkinElmer, Japan) [25].

2.5.2. Fourier transform infrared (FT-IR) analysis

The biomolecules present in *D. aegyptium* aqueous extract, which are responsible for the reduction and stabilization of silver ions present in the solution, resulting in AgNP formation, were identified using an ATR FT-IR (Bruker IR, Japan) spectrophotometer in the transmission range of 4000 cm^{-1} to 400 cm^{-1}.

2.5.3. Scanning electron microscopy (SEM)

The surface morphology of AgNPs-DA was visualized using a scanning electron microscope (Philips CM 200). Particles were deposited on carbon tape, coated with gold using an SPI sputter (in a high-vacuum evaporator), and images were captured at 20 kV.

2.5.4. X-ray diffraction (XRD) analysis

The XRD pattern of dried AgNPs-DA was assessed using an X-ray powder diffractometer (JDX 3532; JEOL, Japan). Using CuKa radiation,

Table 1
The diameter of the inhibition zone of the different AgNPs-DA prepared.

Sample	Zone of inhibition (mm ± SD)			
	S. aureus	*P.* aeruginosa	*K.* pneumoniae	*E. coli*
S1	13 ± 0.23	9 ± 0.54	14 ± 0.34	20 ± 0.57
S2	11 ± 0.4	10 ± 0.5	19 ± 0.4	17 ± 0.2
S3	12 ± 0.57	10 ± 0.75	18 ± 0.43	18 ± 0.65
S4	13 ± 0.1	11 ± 0.4	15 ± 0.4	15 ± 0.5
S5	19 ± 0.0	9 ± 0.0	13 ± 0.0	13 ± 0.0
PE	7 ± 0.55	7 ± 0.05	Nil	Nil
PC	22 ± 0.76	21 ± 0.14	21 ± 0.32	18 ± 0.23
NC	Nil	Nil	Nil	Nil
S6	15 ± 0.23	8 ± 0.85	13 ± 0.76	12 ± 0.6
S7	16 ± 0.84	8 ± 0.45	12 ± 0.56	12 ± 0.4
S8	17 ± 1.04	9 ± 0.65	10 ± 1.15	12 ± 0.74
S9	18 ± 0.76	9 ± 1	11 ± 0.93	13 ± 0.73
S10	19 ± 1.32	10 ± 1.5	18 ± 1.34	15 ± 0.82
PE	7 ± 0.75	7 ± 0.25	Nil	Nil
PC	21 ± 0.5	22 ± 1.3	17 ± 0.2	20 ± 0.4
NC	Nil	Nil	Nil	Nil

PE, plant extract; PC, positive control (erythromycin and amikacin); NC, negative control (water).

Table 2
The composition of the various *D. aegyptium-mediated* silver nanoparticle batches.

Batch	Sample code	Silver nitrate volume (ml)	Extract concentration (%)	Silver nitrate molarity (mM)	Extract volume (ml)
S1	AgNPs-DA1	50	1	10	10
S2	AgNPs-DA 2	50	2	10	10
S3	AgNPs-DA 3	50	3	10	10
S4	AgNPs-DA 4	50	4	10	10
S5	AgNPs-DA 5	50	5	10	10
S6	AgNPs-DA 6	50	5	2.5	10
S7	AgNPs-DA 7	50	5	5	10
S8	AgNPs-DA 8	50	5	7.5	10
S9	AgNPs-DA 9	50	5	10	10
S10	AgNPs-DA 10	50	5	15	10

patterns were recorded at 60 kV voltage, 50 mA current, and 1° per minute scanning rate over a 2θ of 20–60 °C diffraction angle. The crystallite size was calculated using the Scherrer equation: [26]

2.6. Antibacterial activity

The antibacterial activity of the plant extract and AgNPs-DA was determined using the well diffusion method against gram-positive (*S. aureus*) and gram-negative (*E. coli*, *K. pneumoniae,* and *P. aeruginosa*) bacterial strains. Muller-Hinton agar plates loaded with AgNPs-DA, plant extract, deionized water (negative control), and antibiotic discs (positive control) were incubated at 37 °C for 18 h. Diameters of the inhibitory zones (ZOI) around the wells were recorded.

2.7. Synthesis and characteristics of AgNPs-DA-loaded PNG Hydrogel

2.7.1. Synthesis of the hydrogel

For the preparation of blank PVA, Na-alginate, and gelatin-based hydrogel (PNG), a PVA solution (10 %) was prepared by dissolving PVA in a predetermined amount of distilled water under heating at 80 °C with continuous stirring at 100–150 rpm. The solution was cooled to room temperature after preparation. Na-alginate solution (4 %) was prepared by dissolving it in distilled water at 40 °C with constant stirring for 15 min. Gelatin was instantly dissolved in distilled water under constant stirring without heating to obtain a 4 % solution. All three polymer solutions were then combined (PVA:NaAlg:G ratio of 60:20:20), continuously stirred at 500 rpm for an hour, poured into Petri plates, and freeze-thawed for three consecutive cycles [27]. For the preparation of silver nanoparticle-loaded PNG hydrogels, 0.2 g of AgNPs-DA5 was added to the mixture of the polymers (20 ml) with continuous stirring at 500 rpm for 1 hour and freeze-thawed for three consecutive cycles.

2.7.2. Characteristics of the hydrogel

The colour, consistency, and homogeneity of the hydrogels were evaluated visually. FT-IR analysis of blank hydrogels and AgNP-DA-loaded hydrogels was also performed to confirm the compatibility of the nanoparticles with the polymers. The equilibrium swelling behaviour of the hydrogel dressing was estimated by the gravimetric method at pH values of 4, 5.5, 6.5, and 7.5. The dried hydrogel (2 cm × 2 cm) was further dried, weighed, and immersed in 0.5 M USP phosphate buffer at the desired pH. At regular time intervals, the swollen hydrogel was removed from the solution, blobbed with blotting paper, and weighed. The procedure was repeated until no change in weight was observed. The percentage swelling of the hydrogel sample was estimated using the following equation:

$$Swelling(\%) = \frac{w_t - w_d}{w_d}$$

where w_t represents the weight of the swollen hydrogel at time (t), and w_d indicates the initial weight of the dry hydrogel.

2.8. Skin irritation test

A skin irritation test was performed to evaluate the toxicity of the AgNPs-DA-loaded PNG hydrogel on rat skin (Wistar rats) [28]. Two animal groups were tested: an AgNP-DA-loaded hydrogel group and a commercial product (standard) group (n = 5 in each group). After shaving the hair on the dorsal side (5 cm^2 area) with a razor, a piece of hydrogel was placed on the shaved area, and signs of itching, irritation, erythema, and edema were noted at 1, 6, 24, and 48 h.

2.9. In vivo wound healing evaluation

Adult male Wistar rats (145 g) were obtained from the animal house of the Faculty of Pharmacy, Bahauddin Zakariya University, Multan, Pakistan. The study protocol was evaluated and approved by the Pharmacy Ethical Committee for the Use of Laboratory Animals, Faculty of Pharmacy, Bahauddin Zakariya University, Multan, Pakistan (No. 206/PEC/2022). During the study, animals were housed under regulated conditions of controlled temperature (25 °C ± 1), with a 12/12 h light/dark cycle, free access to water, and a standard feed. Rats were randomly divided into four groups (n = 6), anesthetized by applying lignocaine gel to the skin, and shaved on the dorsal side. The shaved area was sanitized with 70 % ethanol, and the skin was incised using a razor to produce a wound approximately 1 cm in length. The rats in Group 1 (control group) were kept untreated. Rats in group 2 (commercial product group) were treated daily with a commercial product containing 1 % silver sulfadiazine. Rats in group 3 (AgNP (1 %) hydrogel group) were treated with the hydrogel formulation applied daily. The size of the wound was measured and photographed on days 0, 3, 7, and 9, and the percentage wound size reduction was estimated using the following equation:

$$\%\text{wound size reduction} = \frac{W_0 - W_d}{W_0} \times 100$$

Where W_0 denotes the wound area on day 0 and W_d denotes the wound size on the day of measurement, such as days 3, 5, 7, and 9.

3. Results and discussion

3.1. Visual observation and UV-spectroscopy

To optimize the green synthesis of AgNPs using *D. aegyptium* aqueous extract, various batches of nanoparticles with varying parameters were synthesized. To determine the effect of plant extract concentration on nanoparticle synthesis, AgNPs-DA1 to AgNPs-DA5 were synthesized with various concentrations of plant extract (1 %, 2 %, 3 %, 4 %, and 5 %) and a constant silver nitrate solution concentration (5 mM). On the other hand, to determine the effect of silver nitrate concentration on nanoparticles, batches AgNPs-DA6 to AgNPs-DA10 with varied concentrations of $AgNO_3$ solution (2.5 mM, 5 mM, 7.5 mM, 10 mM, and 15 mM) and a fixed plant extract concentration (5 %) were synthesized. In all batches, the silver nitrate solution was added to the *D. aegyptium* plant extract, which resulted in a colour change from light yellowish to brownish owing to the excitation of surface plasmon resonance (SPR), indicating the formation of AgNPs (Fig. 1A). The maximum colour change was observed in solutions containing 5 % leaf extract and 10 mM $AgNO_3$ (S5, Table 2). Phytochemicals present in plant extracts are

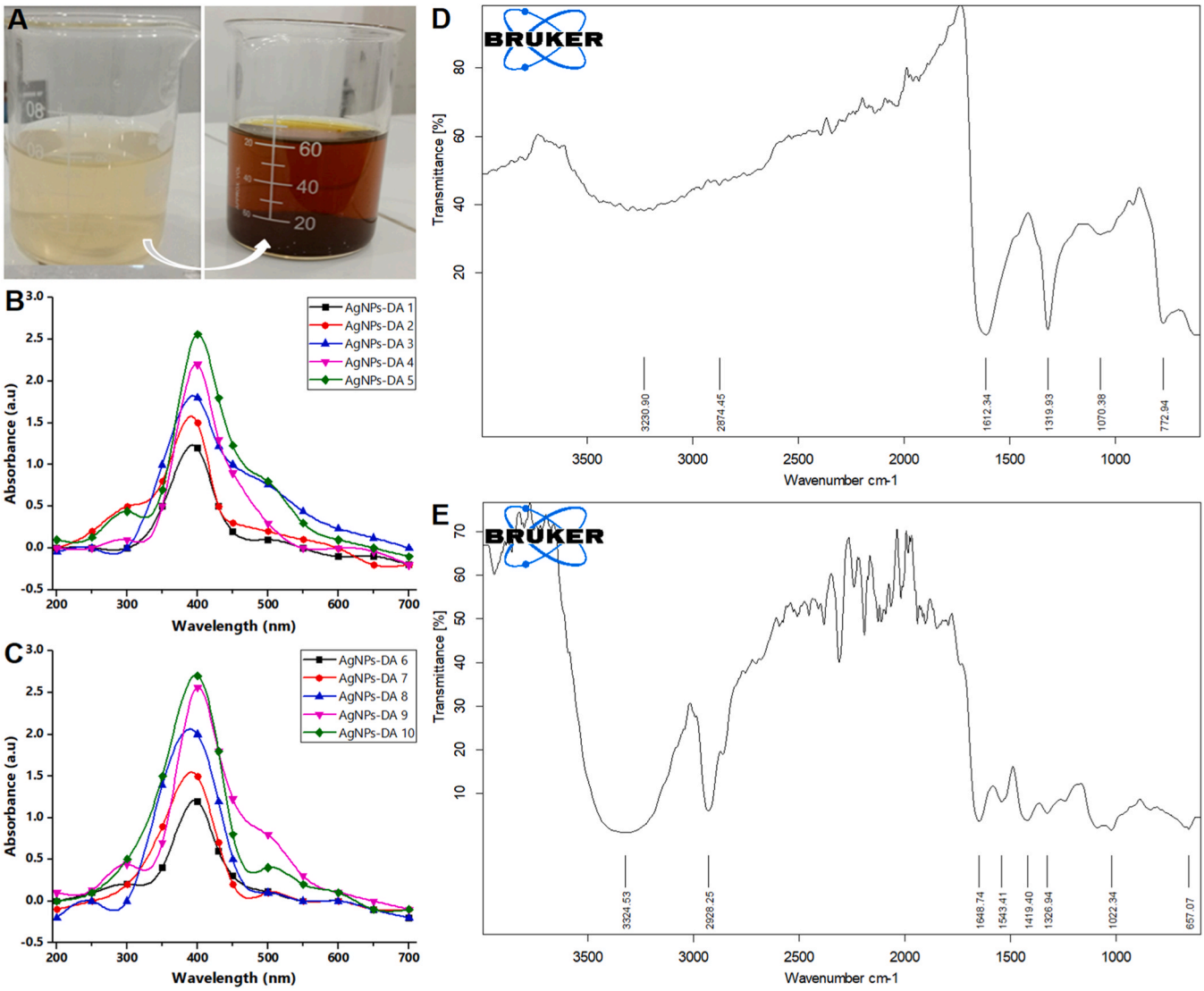

Fig. 1. Effect of formulation concentrations & Fourier-transform infrared spectroscopy (FT-IR) characteristics of AgNPs-DA vs plant extract. (A) Colour change after formation of AgNPs-DA5. (B) Effect of plant extract concentration on the synthesis of AgNPs-DA. (C) Effect of silver nitrate concentration on the synthesis of AgNPs-DA. (D) FT-IR spectra of *D. aegyptium* plant extract. (E) FT-IR spectra of AgNPs-DA5.

thought to reduce silver nitrate [29]. UV–visible spectroscopy exhibited an SPR spectrum around 400 nm (Figs. 1B and 1C). The intensity of the absorption peaks increased with increasing concentrations of both the silver nitrate solution and the plant extract. The high $AgNO_3$ salt concentration provided more ions for the reduction and stabilization of nanoparticles [30]. Similarly, a higher concentration of plant extracts means that more phytochemicals are available for the reduction and stabilization of silver, resulting in a higher nanoparticle yield. Our results are in close agreement with those reported by Saifullah et al. and Yasmin et al. [31,32].

3.2. FT-IR of AgNPs-DA

The phytochemicals present in the *D. aegyptium* plant aqueous extracts are responsible for the capping and stabilization of the biosynthesized nanoparticles [13]. FT-IR spectroscopy was used to identify the functional groups participating in the capping of AgNPs-DA (Figs. 1D and 1E). The broad band obtained around 3230.90 cm^{-1} (Figs. 1D) and 3324.53 cm^{-1} (Fig. 1E) exhibited O-H stretching vibrations associated with alcoholic compounds. The absorption peaks at 2928.25 cm^{-1} in Figs. 1D and 2874.45 cm^{-1} in Fig. 1E are due to stretching in the C-H bonds of aromatic phytochemicals. The peaks at 1648.74 cm^{-1} and 1612.34 cm^{-1} in Figs. 1D and 1E, respectively, may be attributed to N-H asymmetric stretching vibrations. The peaks at 1326.94 cm^{-1} and 1319.93 cm^{-1} in Figs. 1D and 1070.38 cm^{-1} Fig. 1E represent C-O stretching vibrations owing to secondary alcohols. These spectral analyses suggest the involvement of flavonoids and proteins in the plant extract in the reduction and stabilization of the nanoparticles.

3.3. X-ray diffraction

The XRD pattern of dried AgNPs-DA5 (Fig. 2A) showed diffraction peaks at 2θ of 38.53°, 46.61°, 55.19°, and 57.94°° corresponding to the planes (111), (200), (220), and (311), respectively. These patterns reflect the face-centered cubic crystalline nature of the synthesized nanoparticles. Similar results were reported earlier [24]. The average crystallite size was found to be 28.03 nm and was calculated using Scherrer's equation [26].

3.4. SEM analysis

The SEM image of AgNPs-DA5 shows rough particles with a degree of

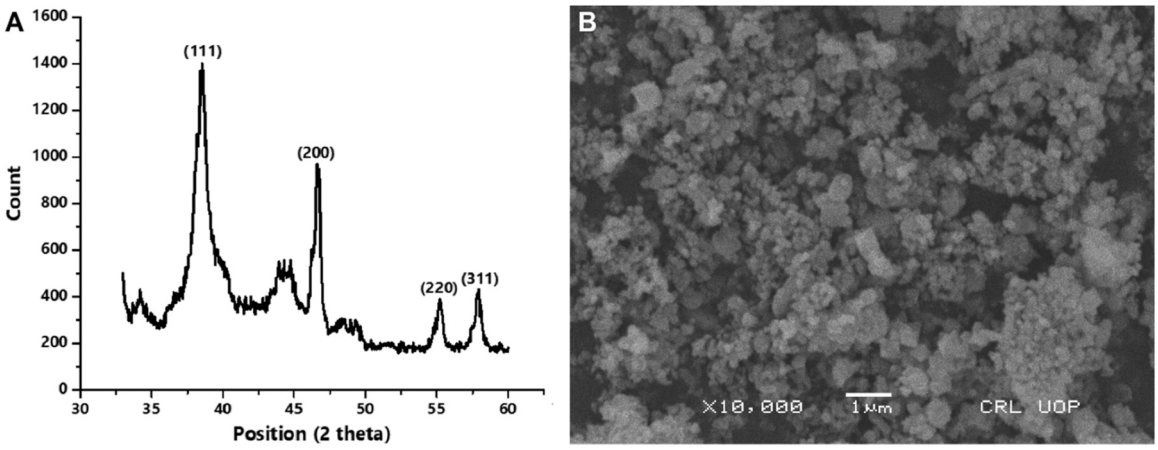

Fig. 2. X-ray diffraction (XRD) and scanning electron microscope (SEM) characteristics of AgNPs. (A) XRD pattern of AgNPs-DA5 and (B) SEM image of Agnes -DA5.

unevenness and irregular shapes in the clusters (Fig. 2B). The appearance of nanoparticles as aggregates or clusters might be due to electrostatic interactions and hydrogen bonds between the bio-organic capping molecules attached to AgNPs-DA [33].

3.5. *In vitro antibacterial activity of AgNPs-DA*

The in vitro antibacterial activity of the synthesized particles is shown in Fig. 3 and Table 1. It can be observed that *D. aegyptium* aqueous plant extract has little antibacterial activity against *S. aureus* and *P. aeruginosa* (Fig. 3 Aii & Bii), with Zones of Inhibition (ZOI) of approximately 7 mm ± 0.65 and 7 ± 0.15, respectively, and no activity against *E. coli* and *K. pneumonia.* However, *D. aegyptium* plant extract-mediated AgNPs showed significant antibacterial activity against all the tested bacterial strains, with ZOIs comparable to that of the positive control. AgNPs-DA10, AgNPs-DA4, AgNPs-DA2, and AgNPs-DA1 showed the largest zones of inhibition (ZOIs) against *S. aureus*, *P. aeruginosa, K. pneumonia,* and *E. coli*, respectively (Table 1).

3.6. *Preparation and characterization of integrated PNG hydrogel*

The ability of hydrogels to take up water is one of the most essential attributes for wound dressing applications [23], creating a moist environment and enhancing the rate of epithelialization at wound sites. In the current study, hydrogels comprising PVA, NaAlg, and gelatin were produced by freeze-thawing cycles for topical application. Freeze–thaw cycles increase the degree of physical cross-linking between the polymers [34]. The blank hydrogels were white in colour (Fig. 4Ai), whereas the silver nanoparticle-loaded hydrogels were dark grey to black in colour (Fig. 4Aii).

The hydrogels showed pH-dependent swelling behaviour (Fig. 4B), exhibiting a quick and sudden increase in percent swelling as the pH increased from 4 to 7 in a short period of half an hour, followed by saturation and then steady swelling over time. The increase in swelling with increasing pH could be due to an increase in the number of ionizable carboxyl groups, causing electrostatic repulsion that leads to swelling of the hydrogels. These results indicated that our PNG hydrogel dressings could swell and release their payloads at and around the pH of the wound and skin environment. In wound healing through hydrogel

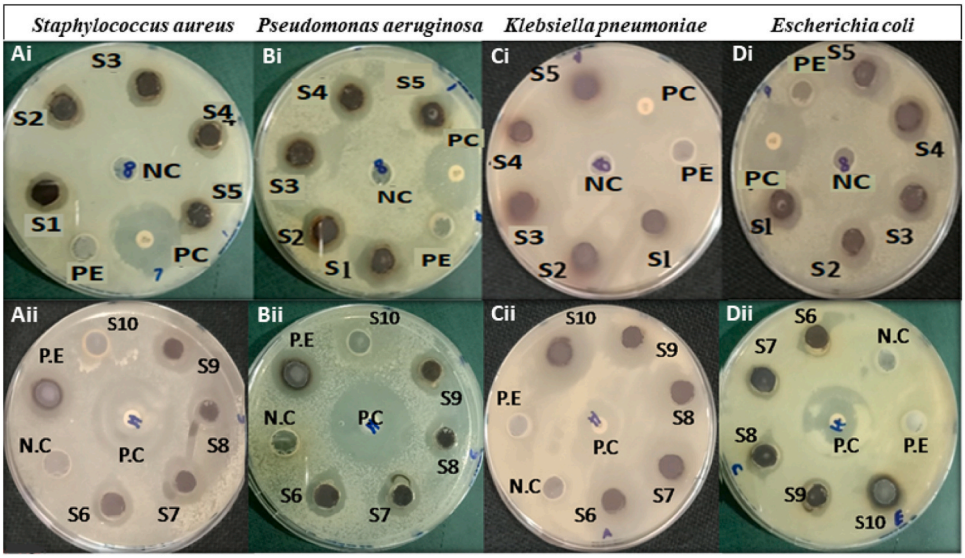

Fig. 3. Antibacterial activity of AgNPs-DA against different bacterial strains. (Ai & Aii), zones of inhibition (ZOI) against *Staphylococcus aureus*; (Bi & Bii), ZOI against *Pseudomonas aeruginosa*; (Ci & Cii), ZOI against *Klebsiella pneumoniae* and (Di & Dii) are ZOI against *Escherichia coli*. S1 = AgNPs-DA1, S2 = AgNPs-DA2, S3 = AgNPs-DA3, S4 = AgNP-DA4, S5 = AgNP-DA5, S6 = AgNPs-DA6, S7 = AgNPs-DA7, S8 = AgNPs-DA8, S9 = AgNP-DA9, and S10 = AgNP-DA10. NC = negative control (water), PC = positive control (erythromycin and amikacin), and PE = plant extract.

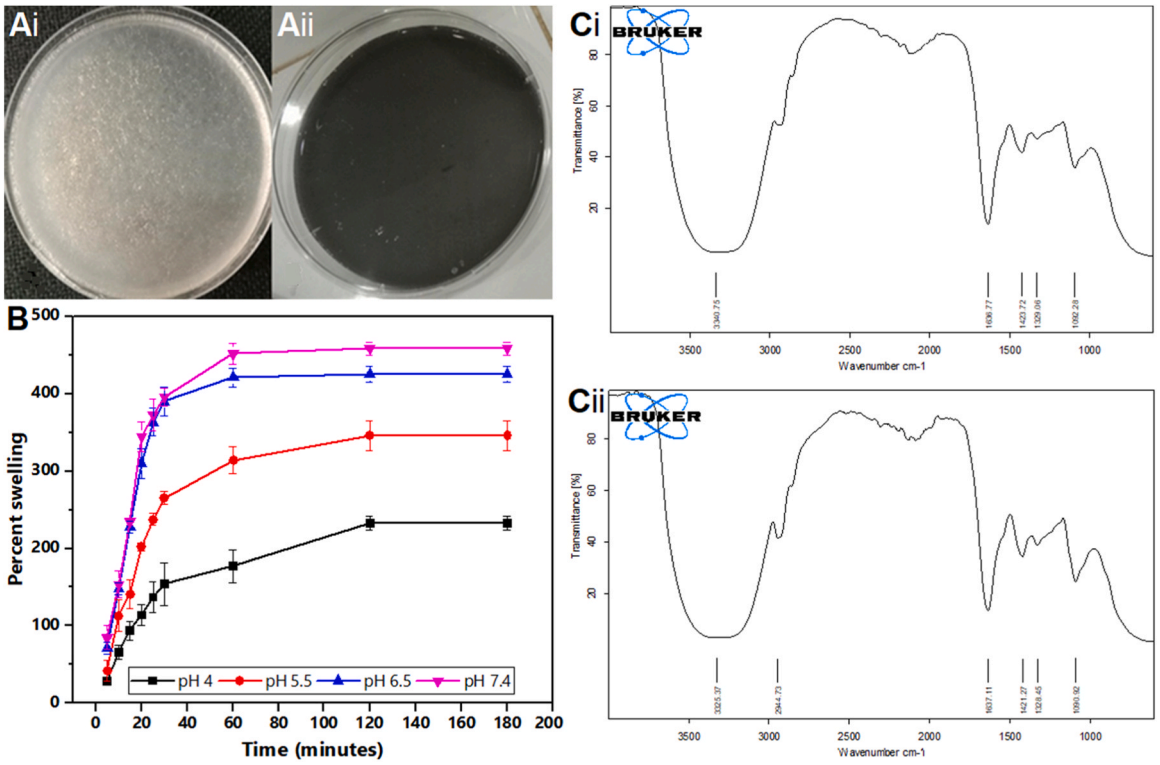

Fig. 4. Blank and AgNPs-loaded hydrogels & their characteristics. (Ai) and (Aii) blank and AgNPs-DA5-loaded PNG (PVA, Na-Alginate, and gelatin) hydrogels, respectively. (B) Swelling behaviour of PNG hydrogels at various physiological pH values. (Ci) and (Cii) FT-IR of blank and AgNPs-DA5-loaded PNG hydrogels, respectively.

dressings, optimum water absorption is desirable, as a high degree of water uptake might hamper the otherwise faster rate of healing and re-epithelialization [4]. Our hydrogel dressings showed accelerated wound healing (as discussed in the next section, 2.7), indicating optimum water absorption for effective wound healing in an animal model.

FT-IR spectra of the blank hydrogel (Fig. 4 Ci) and silver nanoparticles-loaded hydrogel formulation (Fig. 4Cii) showed bands around 3340.75 cm^{-1} and 3277.57 cm^{-1} respectively, indicating OH stretches. The peaks at 1636.77 cm^{-1} indicate NH bending. The bands at approximately 1637 cm^{-1} and 1421 cm^{-1} indicate amide carbonyl vibrations. The presence of amino, carboxyl, and hydroxyl groups is responsible for electrostatic interactions and hydrogen bonding among polymers [35], resulting in consistent and flexible hydrogel dressings that allow adherence to the skin. The FTIR spectra of the blank and AgNP-loaded hydrogels showed no significant change in the major peaks, indicating the absence of any chemical interaction between the silver nanoparticles and polymers.

3.7. *In vivo wound healing study*

Before the evaluation of AgNPs-DA-loaded hydrogel dressings for wound healing capacity in an animal wound model, the hydrogel formulation was tested for skin irritation first. Skin irritation is a localized inflammatory response that occurs immediately after

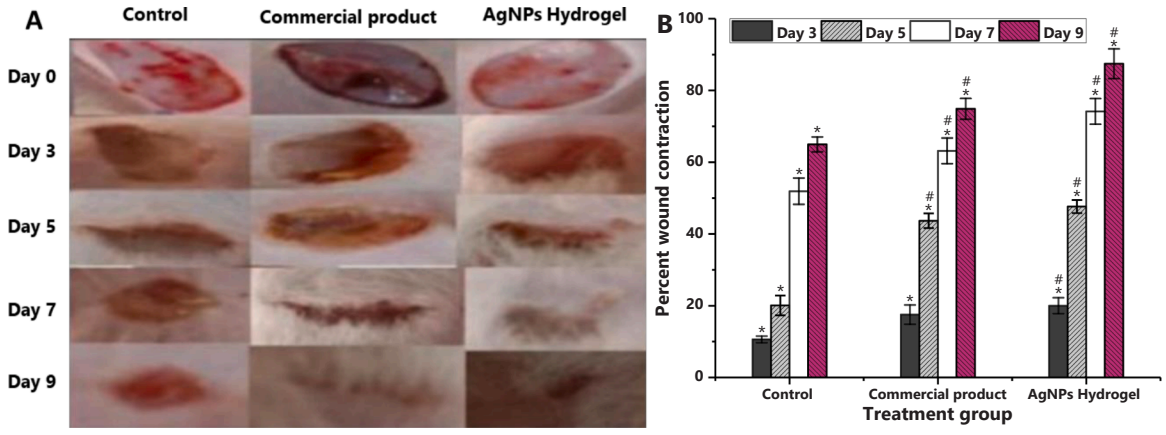

Fig. 5. Wound healing activity of AgNPs-loaded hydrogel against control & a commercial product. (A) Photographs of wounds for the different animal groups on the different measurement days. The control group received no treatment, the group received commercial treatment (1 % silver sulfadiazine), and the group received AgNPs-DA-loaded (1 %) hydrogel dressing. (B) percent wound contraction. Data are expressed as mean ± SD. * denotes statistical comparison for the control group vs. standard group and AgNPs-DA hydrogel group, whereas # denotes comparison for the standard group vs. AgNPs-DA hydrogel group (* and # indicate statistically significant differences).

stimulation, and is clinically identified as erythema, oedema, itching, and discomfort [36]. No signs of redness, swelling, or itching were observed upon application of the PNG hydrogel dressing, indicating the biocompatibility of the hydrogel dressings with no harmful effects on skin cells.

The wound-healing capacity of the AgNPs-DA-loaded hydrogel dressings was evaluated over 9 days. Fig. 5A illustrates a gradual decrease in wound size over time in all the groups. Wound diameters were measured as part of the quantitative examination of wound healing on 0, 3rd, 5th, 7th and 9th days, and the percent wound contraction was estimated (Fig. 5B). The percentage of wound contraction in the control group was 10.59 % ± 0.916, 20.07 % ± 2.75, 51.90 % ± 3.65, and 65.51 % ± 2.06 on the 3rd, 5th, 7th and 9th days, respectively, which was the slowest among all experimental groups. The rats in group 2 (the commercial product group), which were treated with the commercial product Quench cream (1 % w/w silver sulfadiazine), showed wound contractions of 17.50 % ± 2.69, 43.67 % ± 2.04, 63.16 % ± 3.56, and 74.85 % ± 2.92 on the 3rd,5th,7th and 9th days, respectively. Group 3 rats (AgNP hydrogel group), which were dressed with the AgNPs-DA-loaded PNG hydrogel formulation (1 %) on a daily basis, showed wound healing percentages of 19.98 % ± 2.19, 47.65 % ± 1.82, 74.14 % ± 3.58, and 87.44 ± 4.12 on the 3rd, 5th, 7th, and 9th days, respectively. These results indicated that wound healing was significantly better in groups 2 and 3 than in rats in the control group. On day 3, although the percent wound contraction in the hydrogel group (group 3) was slightly better than that in the commercial product group, the difference was statistically insignificant ($p < 0.05$). On days 5, 7, and 9 of the study, wound healing was significantly accelerated in the group treated with the hydrogel formulation compared to that in the commercial product group ($p < 0.05$). The highest wound closure was observed on day 9 in Group 3, with a marked decrease in wound diameter, almost complete re-epithelization, and evidence of keratinization (Fig. 5). These results suggest that an optimum level of moisture was present on the wound, and the release of AgNPs-DA from the hydrogel dressing created an ideal environment for accelerated regeneration of epithelial cells. The presence of moisture maintains an electrical gradient between the wound and the surrounding area of the skin, which may stimulate epidermal migration [37]. The matrix formed by blending polymers manifests an efficient haemostatic effect, which renders hydrogels an effective wound dressing material [38]. The rats in all groups survived the study period, with no evidence of necrosis, inflammation, or haemorrhage. In the current study, PNG hydrogels loaded with AgNPs-DA greatly improved wound healing compared to conventional product (commercial). Application of the formulated hydrogel dressing on the surface of wounds might act as a biomechanical barrier, which is a great advantage, as well as exhibiting antibacterial activity. The antibacterial effect of Ag has been associated with its ability to interact with bacterial plasma membranes, proteins, and enzymes involved in vital cellular processes, such as the electron transport chain [39]. The silver nanoparticles formulated in this study, along with other recently reported greenly synthesized metallic nanoparticles, such as iron, palladium, copper, and gold-pectin-iron nanocomposites [40-43], could serve as potential new therapeutic agents in real life.

4. Conclusion

This study aimed to formulate safe, cost-effective, and biocompatible AgNP-based hydrogel dressings for wound healing. The biologically produced nanoparticles using a plant extract involved simple, sustainable, and environmentally friendly methodology without the use of organic solvents. FT-IR analysis confirmed the caping effect of the used plant extract. The synthesized nanoparticles were crystalline in nature, with an average crystallite size of 28.03 nm. The optimal nanoparticle synthesis conditions were found to be 10 mM $AgNO_3$ solution, which provided more ions for particle stabilization, and 5 % plant extract concentration, which resulted in a higher nanoparticle yield. AgNPs-DA have demonstrated antibacterial activity in vitro against *S. aureus*, *P. aeruginosa*, *K. pneumoniae,* and *E. coli*, which is advantageous because open wounds are more prone to bacterial infections. The formulated hydrogels containing AgNPs-DA (1 %) showed promising wound healing ability in a rodent model. Our study suggests that the AgNPs-DA-incorporated hydrogel dressing is a novel product with potential implications for wound treatment.

Financial disclosure

No specific funding was received to conduct this research work.

CRediT authorship contribution statement

Sana Nayab: Methodology, Investigation, Formal analysis, Data curation. **Maryam Zain:** Visualization, Methodology, Data curation, Conceptualization. **Hina Raza:** Visualization, Validation, Software, Resources. **Mohamed Deifallah Yousif:** Writing – review & editing, Validation, Software, Formal analysis. **Zermina Rashid:** Writing – review & editing, Writing – original draft, Resources, Project administration, Conceptualization. **Ambreen Aleem:** Writing – review & editing, Formal analysis, Data curation.

Declaration of Competing Interest

The authors declare that they have no known competing financial interests or personal relationships that could have appeared to influence the work reported in this paper.

Data availability

No data was used for the research described in the article.

Acknowledgment

All authors are thankful to Women University Multan and the Faculty of Pharmacy Bahauddin Zakariya University Multan for providing technical support.

References

[1] A. A. A, N. S. T. Usama Farghaly Aly,Heba A Abou-Taleb, Formulation and evaluation of simvastatin polymeric nanoparticles loaded in hydrogel for optimum wound healing purpose, Drug Des. Devel Ther. vol. 13 (2019) 1567–1580, doi: doi.org/10.2147/DDDT.S198413.
[2] L.G. Ovington, Advances in wound dressings, Clin. Dermatol. vol. 25 (2007) 33–38, https://doi.org/10.1016/j.clindermatol.2006.09.003.
[3] D. Zhang, et al., Carboxyl-modified poly(vinyl alcohol)-crosslinked chitosan hydrogel films for potential wound dressing, Carbohydr. Polym. vol. 125 (2015) 189–199, https://doi.org/10.1016/j.carbpol.2015.02.034.
[4] H.-G.C. Jong Oh Kim, Jun Young Choi, Jung Kil Park, Jeong Hoon Kim, Sung Giu Jin, Sun Woo Chang, Dong Xun Li, Ma-Ro Hwang, Jong Soo Woo, Jung-Ae Kim, Won Seok Lyoo, Chul Soon Yong, Development of clindamycin-loaded wound dressing with polyvinyl alcohol and sodium alginate, Biol. Pharm. Bull. vol. 31 (12) (2008) 2277–2282.
[5] N.Y. Lee, W.C. Ko, P.R. Hsueh, Nanoparticles in the treatment of infections caused by multidrug-resistant organisms, Front Pharm. vol. 10 (2019) 1–10, https://doi.org/10.3389/fphar.2019.01153.
[6] J. Li, et al., A new formulation of Ni/Zn bi-metallic nanocomposite and evaluation of its applications for pollution removal, photocatalytic, electrochemical sensing, and anti-breast cancer, Environ. Res. vol. 233 (2023) 116462, https://doi.org/10.1016/j.envres.2023.116462.
[7] H. Ma, et al., Green decorated gold nanoparticles on magnetic nanoparticles mediated by Calendula extract for the study of preventive effects in streptozotocin-induced gestational diabetes mellitus rats, Inorg. Chem. Commun. vol. 151 (2023) 110633, https://doi.org/10.1016/j.inoche.2023.110633.
[8] A. Dehnoee, R. Javad Kalbasi, M.M. Zangeneh, M.R. Delnavazi, A. Zangeneh, One-step synthesis of silver nanostructures using Heracleum persicum fruit extract, their cytotoxic activity, anti-cancer and anti-oxidant activities, Micro Nano Lett. vol. 18 (1) (2023) 1–11, https://doi.org/10.1049/mna2.12153.
[9] H. Zong, et al., Synthesis of Fe 3 O 4 nanoparticles encapsulated with orange pectin for the treatment of gastrointestinal cancers, Mater. Express vol. 12 (12) (2023) 1455–1464, https://doi.org/10.1166/mex.2022.2314.

[10] V. Kumar, S.K. Yadav, Plant-mediated synthesis of silver and gold nanoparticles and their applications, J. Chem. Technol. Biotechnol. vol. 84 (2009) 151–157, https://doi.org/10.1002/jctb.2023.
[11] F. Ahmad, N. Ashraf, T. Ashraf, R.Bin Zhou, D.C. Yin, Biological synthesis of metallic nanoparticles (MNPs) by plants and microbes: their cellular uptake, biocompatibility, and biomedical applications, Appl. Microbiol Biotechnol. vol. 103 (7) (2019) 2913–2935, https://doi.org/10.1007/s00253-019-09675-5.
[12] S. Mathew, Phytonanotechnology: A historical perspective, current challenges, and prospects. in *Phytonanotechnology*, Elsevier Inc, 2020, pp. 1–20, https://doi.org/10.1016/B978-0-12-822348-2.00001-2.
[13] M. Noruzi, Biosynthesis of gold nanoparticles using plant extracts, Bioprocess Biosyst. Eng. vol. 38 (1) (2015) 1–14, https://doi.org/10.1007/s00449-014-1251-0.
[14] Y.Y. Loo, et al., In Vitro antimicrobial activity of green synthesized silver nanoparticles against selected Gram-negative foodborne pathogens, Front Microbiol vol. 9 (JUL) (2018) 1–7, https://doi.org/10.3389/fmicb.2018.01555.
[15] H.X. Li Xu, Yi-Yi Wang, Jie Huang, Chun-Yuan Chen, Zhen-Xing Wang, Silver nanoparticles: synthesis, medical applications and biosafety, Theranostics vol. 10 (20) (2020) 8996–9031, https://doi.org/10.7150/thno.45413.
[16] A.F. Essa, et al., Prevalence of diterpenes in essential oil of euphorbia mauritanica L.: detailed chemical profile, antioxidant, cytotoxic and phytotoxic activities, Chem. Biodivers. vol. 18 (7) (2021), https://doi.org/10.1002/cbdv.202100238.
[17] A.E. Al-snafi, The pharmacological potential of Dactyloctenium aegyptium - A review, Indo Am. J. Pharm. Sci. vol. 4 (2017) 153–159, doi: http://doi.org/10.5281/zenodo.292965.
[18] H. Ye, J. Cheng, K. Yu, In situ reduction of silver nanoparticles by gelatin to obtain porous silver nanoparticle/chitosan composites with enhanced antimicrobial and wound-healing activity, Int. J. Biol. Macromol. vol. 121 (2019) 633–642, https://doi.org/10.1016/j.ijbiomac.2018.10.056.
[19] S.J. Lim, et al., Effect of sodium carboxymethylcellulose and fucidic acid on the gel characterization of polyvinylalcohol-based wound dressing, Arch. Pharm. Res. vol. 33 (7) (2010) 1073–1081, https://doi.org/10.1007/s12272-010-0714-3.
[20] Y.K. Choi, et al., Amniotic membrane extract-loaded double-layered wound dressing: evaluation of gel properties and wound healing, Drug Dev. Ind. Pharm. vol. 40 (7) (2014) 852–859, https://doi.org/10.3109/03639045.2013.788015.
[21] G. Coşkun, E. Karaca, M. Ozyurtlu, S. Özbek, A. Yermezler, I. Çavuşoğlu, Histological evaluation of wound healing performance of electrospun poly(vinyl alcohol)/sodium alginate as wound dressing in vivo, Biomed. Mater. Eng. vol. 24 (2) (2014) 1527–1536, https://doi.org/10.3233/BME-130956.
[22] P. Severino, C.F. da Silva, L.N. Andrade, D. de Lima Oliveira, J. Campos, E.B. Souto, Alginate nanoparticles for drug delivery and targeting, Curr. Pharm. Des. vol. 25 (11) (2019) 1312–1334, https://doi.org/10.2174/1381612825666190425163424.
[23] U.Y. Sevinc Ilkar Erdagi, Fahanwi Asabuwa, Ngwabebhoh, Genipin crosslinked gelatin-diosgenin-nanocellulose hydrogels for potential wound dressing and healing applications, Int. J. Biol. Macromol. vol. 149 (2020) 651–663.
[24] G. Chinnasamy, S. Chandrasekharan, T.W. Koh, S. Bhatnagar, Synthesis, characterization, antibacterial and wound healing efficacy of silver nanoparticles from Azadirachta indica, Front Microbiol vol. 12 (February) (2021) 1–14, https://doi.org/10.3389/fmicb.2021.611560.
[25] N. Mohamed, N.G. Madian, Evaluation of the mechanical, physical and antimicrobial properties of chitosan thin films doped with greenly synthesized silver nanoparticles, Mater. Today Commun. vol. 25 (2020) 101372, https://doi.org/10.1016/j.mtcomm.2020.101372.
[26] K. Jemal, S. P, B.V. Sandeep, Synthesis, characterization, and evaluation of the antibacterial activity of allophylus serratus leaf and leaf derived callus extracts mediated silver nanoparticles, J. Nanomater. (2017), https://doi.org/10.1155/2017/4213275.
[27] M.-C.Y. Mei-Hua Huang, Evaluation of glucan/poly(vinyl alcohol) blend wound dressing using rat models, Int. J. Pharm. vol. 346 (2008) 38–46, https://doi.org/10.1016/j.ijpharm.2007.06.021.
[28] M. Najwa, M.A. Mohd.Cairul, P. Manisha, A. Naveed, R. Nor.Fadilah, Bacterial cellulose/acrylic acid hydrogel synthesized via electron beam irradiation: accelerated burn wound healing in an animal model, Carbohydr. Polym. vol. 114 (2014) 312–320, doi: https://doi.org/10.1016/j.carbpol.2014.08.025.
[29] V. Cittrarasu, et al., Biological mediated Ag nanoparticles from Barleria longiflora for antimicrobial activity and photocatalytic degradation using methylene blue, Artif. Cells Nanomed. Biotechnol. vol. 47 (1) (2019) 2424–2430, https://doi.org/10.1080/21691401.2019.1626407.
[30] M. Amin, F. Anwar, M.R.S.A. Janjua, M.A. Iqbal, U. Rashid, Green synthesis of silver nanoparticles through reduction with Solanum xanthocarpum L. berry extract: Characterization, antimicrobial and urease inhibitory activities against Helicobacter pylori, Int. J. Mol. Sci. vol. 13 (8) (2012) 9923–9941, https://doi.org/10.3390/ijms13089923.
[31] S. Ahmed, Saifullah, M. Ahmad, B.L. Swami, S. Ikram, Green synthesis of silver nanoparticles using Azadirachta indica aqueous leaf extract, J. Radiat. Res. Appl. Sci. vol. 9 (1) (2016) 1–7, https://doi.org/10.1016/j.jrras.2015.06.006.
[32] M. Asif, R. Yasmin, R. Asif, A. Ambreen, M. Mustafa, S. Umbreen, Green synthesis of silver nanoparticles (AgNPs), structural characterization, and their antibacterial potential, Dose-Response vol. 20 (1) (2022) 1–11, https://doi.org/10.1177/15593258221088709.
[33] V. B. & G. R. Muthu Thiruvengadam, Ill-Min Chung, Thandapani Gomathi, Mohammad Azam Ansari, Venkatesan Gopiesh Khanna, Synthesis, characterization and pharmacological potential of green synthesized copper nanoparticles, Bioprocess Biosyst. Eng. vol. 42 (2019) 1769–1777, https://doi.org/10.1007/s00449-019-02173-y.
[34] H. C. M, P. N. A, Structure and morphology of freeze / thawed PVA hydrogels, Macromolecules vol. 33 (2000) 2472–2479, doi: https://doi.org/10.1021/ma9907587.
[35] Y. Li, H. Jia, Q. Cheng, F. Pan, Z. Jiang, Sodium alginate-gelatin polyelectrolyte complex membranes with both high water vapor permeance and high permselectivity, J. Memb. Sci. vol. 375 (1–2) (2011) 304–312, https://doi.org/10.1016/j.memsci.2011.03.058.
[36] N. Haridas, M.J. Rosemary, Effect of steam sterilization and biocompatibility studies of hyaluronic acid hydrogel for viscosupplementation, Polym. Degrad. Stab. vol. 163 (2019) 220–227, https://doi.org/10.1016/j.polymdegradstab.2019.03.019.
[37] M. Ramos-e-Silva, M.C.R. de Castro, New dressings, including tissue-engineered living skin, Clin. Dermatol. vol. 20 (2002) 715–723, doi: https:https://doi.org/10.1016/S0738-081X(02)00298-5.
[38] T. Coviello, P. Matricardi, C. Marianecci, F. Alhaique, Polysaccharide hydrogels for modified release formulations, J. Con Rel vol. 119 (1) (2007) 5–24, https://doi.org/10.1016/j.jconrel.2007.01.004.
[39] M.D.D.Thirumurugan Gunasekaran, Tadele Nigusse, Silver nanoparticles as real topical bullets for wound healing, J. Am. Col. Clin. Wou Spec. vol. 3 (4) (2012) 82–96, https://doi.org/10.1016/j.jcws.2012.05.001.
[40] Z. Shi, et al., Cu immobilized on chitosan-modified iron oxide magnetic nanoparticles: preparation, characterization and investigation of its anti-lung cancer effects, Ara J. Chem. vol. 14 (2021) 103224, https://doi.org/10.1016/j.arabjc.2021.103224.
[41] M. Shahriari, et al., Palladium nanoparticles decorated Chitosan-Pectin modified Kaolin: It's catalytic activity for Suzuki-Miyaura coupling reaction, reduction of the 4-nitrophenol, and treatment of lung cancer, Inorg. Chem. Commun. vol. 141 (no.) (2022) 109523, https://doi.org/10.1016/j.inoche.2022.109523.
[42] J. Bai, X. Gongsun, L. Xue, M.M. Zangeneh, Introducing a modern chemotherapeutic drug formulated by iron nanoparticles for the treatment of human lung cancer, J. Exp. Nanosci. vol. 16 (1) (2021) 398–410, https://doi.org/10.1080/17458080.2021.1998460.
[43] Y. Li, N. Li, W. Jiang, G. Ma, M.M. Zangeneh, In situ decorated Au NPs on pectin-modified Fe3O4 NPs as a novel magnetic nanocomposite (Fe3O4/Pectin/Au) for catalytic reduction of nitroarenes and investigation of its anti-human lung cancer activities, Int. J. Biol. Macromol. vol. 163 (2020) 2162–2171, https://doi.org/10.1016/j.ijbiomac.2020.09.102.